

# Understanding and improving the Effective Mass for LHC searches

---

**Maria Eugenia Cabrera**

*University of Amsterdam  
Institute of Theoretical Physics  
GRAPPA  
E-mail: [M.E.CabreraCatalan@uva.nl](mailto:M.E.CabreraCatalan@uva.nl)*

**J. Alberto Casas**

*Instituto de Física Teórica, IFT-UAM/CSIC  
U.A.M., Cantoblanco,  
28049 Madrid, Spain  
E-mail: [alberto.casas@uam.es](mailto:alberto.casas@uam.es)*

**ABSTRACT:** A handy and extensively used kinematic variable in LHC analyses, especially for golden SUSY signals of multijets plus missing energy, is the Effective Mass,  $M_{\text{eff}} = \sum_j |p_T^j| + |p_T^{\text{miss}}|$ . Empirically, the value of  $M_{\text{eff}}$  at which the histogram of events has a maximum is correlated with the SUSY spectrum,  $M_{\text{eff}}|_{\text{max}} \simeq 80\% M_{\text{susy}}$ , where  $M_{\text{susy}}$  is essentially the sum of the masses of the SUSY particles initially created. In this paper we explain the reason for such strong correlation, pointing out the cases where the correlation is not good. Besides, we propose a new variable, the Effective Transverse Energy,  $\mathcal{E}_T^{\text{eff}}$ , which shows an even better and more direct correlation  $\mathcal{E}_T^{\text{eff}}|_{\text{max}} \simeq M_{\text{susy}}$ , and is independent of the procedure followed to identify the jets.  $\mathcal{E}_T^{\text{eff}}$  and  $M_{\text{eff}}$  are complementary variables, rather than competitors; and plotting histograms in both can be useful to cross-check the results, allowing a better and more robust identification of  $M_{\text{susy}}$ . The extension of this procedure to other scenarios of new physics (not necessarily SUSY) is straightforward.

**KEYWORDS:** Beyond Standard Model, Supersymmetry Phenomenology, Supersymmetry Searches, Kinematic Variables, LHC.

---

## Contents

<b>1. Introduction</b>	<b>1</b>
<b>2. Strategy for the kinematic analysis</b>	<b>3</b>
2.1 W boson production in $p\bar{p}$ colliders	3
2.2 Pair production of SUSY particles at LHC	6
<b>3. Understanding the correlation <math>M_{\text{susy}} - M_{\text{eff}}</math></b>	<b>8</b>
<b>4. Proposal of a new kinematic variable, <math>\mathcal{E}_T^{\text{eff}}</math></b>	<b>10</b>
<b>5. Testing the efficiency of <math>M_{\text{eff}}</math> and <math>\mathcal{E}_T^{\text{eff}}</math> in assorted SUSY models</b>	<b>11</b>
<b>6. Conclusions</b>	<b>16</b>
<b>7. Appendix</b>	<b>17</b>

---

## 1. Introduction

The LHC is already probing new physics beyond the reach of past experiments. There are two main questions to address: 1) Is there any signal of New Physics (NP)? and 2) In the positive case, which NP is it? In order to optimize the answer to these questions there is an intense activity to explore assorted strategies for the search of NP. The task is challenging, due in part to the fact that LHC data, though very rich, are not as clean as those from an  $e^+e^-$  collider.

Supersymmetry (SUSY) is one of the few candidates for physics beyond the SM that is really well motivated from the theoretical point of view and allows to perform detailed calculations and thus realize precise predictions. Indeed SUSY has been the most extensively studied candidate for new physics in the last decades and the first LHC analyses are using SUSY as a paradigmatic scenario of new physics to present their constraints on physics beyond the SM. Of course, this does not mean that SUSY is really there, but clearly is a most serious scenario to be considered in the light of the LHC.

In the framework of SUSY and under the assumption that superparticles are light enough to be produced and detected at LHC, one can expect a typical signal of multijets

and large missing energy with or without leptons. Searches using channels with leptons in the final state allow quite clean reconstructions. Looking for end-points and using ingenious kinematic variables [1, 2, 3, 4, 5, 6, 7, 8, 9, 10, 11], one can determine in some cases the mass of the sparticle produced in the decay chain. On the other hand, the channel with zero leptons tends to be the golden one producing signals beyond the Standard Model. However, here the analysis becomes much more complicated and the correct identification and reconstruction of the properties of the final states is quite tough. Besides, the separation of the decay chains is normally not possible.

In this context, the use of appropriate kinematic variables and the choice of optimal cuts are instrumental to maximize the SUSY signal from the Standard Model background. But, for the multijet channel, finding the optimal choice is a difficult task. In ATLAS analyses the Effective Mass variable ( $M_{\text{eff}}$ ) plays a very important role [12, 13, 14]. It is defined as,

$$M_{\text{eff}}^{(4)} = \sum_{j=1}^4 |p_T^j| + |p_T^{\text{miss}}|, \quad (1.1)$$

where  $p_T^j$  is the transverse component of the momentum of the four hardest jets [thus the superscript (4)] and  $p_T^{\text{miss}}$  is the missing transverse momentum.

It was found in [15] (from now on HPSSY) that for the Constrained Minimal Supersymmetric Standard Model (CMSSM) there is an outstanding correlation between the value of  $M_{\text{eff}}^{(4)}$  at which the histogram of events has a maximum and the supersymmetric mass  $M_{\text{susy}}$  defined as the minimum of the squark and gluino masses,

$$M_{\text{susy}}^{(\text{HPSSY})} = \min\{m_{\tilde{q}}, m_{\tilde{g}}\}. \quad (1.2)$$

More precisely, HPSSY showed that systematically  $M_{\text{eff}}^{(4)}|_{\text{max}} \simeq 1.9 M_{\text{susy}}^{(\text{HPSSY})}$  for a large collection of CMSSM models with assorted values of the initial supersymmetric parameters. This is very remarkable. However there are some caveats:

1. As admitted by HPSSY the definition of the supersymmetric mass as in eq.(1.2) was rather arbitrary. Although typically the production of a pair of the lightest supersymmetric particles (among squarks and gluinos) is favoured, the production of other pairs, like squark-gluino, can be very frequent too. A refined definition of  $M_{\text{susy}}$  was proposed in [16], namely the sum of all supersymmetric masses weighted by the production cross section (normalized to one) of each one. In this way, the correlation behaves even better, though since the new  $M_{\text{susy}}$  is slightly larger the above number 1.9 decreases somewhat.
2. On the other hand,  $M_{\text{eff}}^{(4)}$  is also smaller than the total effective mass,  $M_{\text{eff}}$ . A more compelling definition, from the theoretical perspective, would be to sum in eq.(1.1) over all jets (surviving certain cuts); though this might be problematic from a practical point of view.

3. So far there is no theoretical explanation for the strong correlation found between the effective mass and the supersymmetric mass. In ref.[15] it is presented as an empirical fact. Certainly, for events with large transverse momenta, one would expect the effective mass to be of the order of sum of the masses of the supersymmetric particles initially created. However, it is not clear why the maximum number of events is always reached at a value of the effective mass so strongly correlated (but slightly smaller) to that sum.
4. As a matter of fact, it was shown in [16] that for more generic MSSM models (beyond the CMSSM) such correlation fails in many instances. Again, it would be very useful to know the reason for that, in order to avoid flawed analyses and improve general strategies.

In the present paper we will offer an explanation for the above points (3) and (4). This understanding will allow us to propose a new kinematic variable, alternative to the effective mass, which shows an even better correlation with the supersymmetric masses, and can be used as an alternative or complementary check in multijet studies at LHC. The discussion and proposal presented here can be easily extrapolated to other scenarios of New Physics different from SUSY.

In section 2 we introduce some relevant kinematic concepts and establish an analogy between the production of the  $W$  boson and that of Supersymmetric particles in hadron colliders. In section 3 we explain the empirical strong correlation between  $M_{\text{eff}}$  and  $M_{\text{susy}}$ . In section 4 we propose a new kinematic variable,  $\mathcal{E}_T^{\text{eff}}$ , which shows an even more robust correlation with  $M_{\text{susy}}$ . In section 5 we test the efficiency of  $M_{\text{eff}}$  and  $\mathcal{E}_T^{\text{eff}}$ , and compare their behaviour using signal simulations at the LHC.

## 2. Strategy for the kinematic analysis

### 2.1 $W$ boson production in $p\bar{p}$ colliders

We start by briefly reviewing the  $W$  boson production and decay in a  $p\bar{p}$  collider, since it is the simplest case involving visible and invisible particles, and it is therefore a useful guide to introduce some notation and some relevant kinematic concepts which will be used later on.

In a  $p\bar{p}$  collider the main process for  $W$  boson production is through quark-antiquark annihilation. Of course, the laboratory (LAB) system of reference does not coincide in general with the center-of-mass (CM) one, since it is affected by boosts, mainly along the collision line ( $z$ ). In addition, there can be less important boosts along a transverse direction due to other effects; in particular, the quarks in initial state may radiate soft gluons (some of them energetic enough to be detected as jets), but for the moment we will ignore these effects.

The  $W$  boson mass is measured by analyzing its leptonic decay  $q\bar{q} \rightarrow W \rightarrow e\bar{\nu}$ , see Fig.1. From the energy and momentum of the electron and the (anti)neutrino, one can

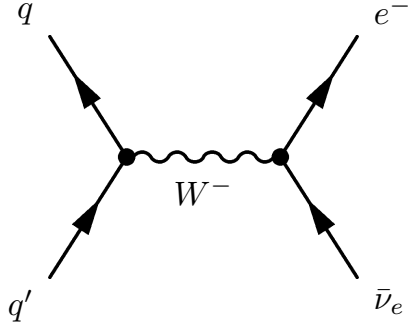


**Figure 1:** Feynman diagram of  $W$ -boson production and decay at hadron colliders.

derive the invariant mass of the  $W$  boson,

$$\begin{aligned} M_W^2 &= M_{\text{inv}}^2 = (E^e + E^\nu)^2 - (\vec{p}^e + \vec{p}^\nu)^2 \\ &= m_e^2 + m_\nu^2 + 2 [E_T^e E_T^\nu \cosh(y^e - y^\nu) - \vec{p}_T^e \cdot \vec{p}_T^\nu] , \end{aligned} \quad (2.1)$$

where  $p_T^a$  is the transverse component of the 3-momentum of the  $a$ -particle, while  $E_T^a$  and  $y^a$  are respectively its transverse energy and rapidity, defined as

$$(E_T^a)^2 = m_a^2 + (p_T^a)^2 = (E^a)^2 - (p_z^a)^2 , \quad y^a = \frac{1}{2} \ln \left( \frac{E^a + p_z^a}{E^a - p_z^a} \right) . \quad (2.2)$$

Note that  $E_T^a$  is invariant under boosts in the  $z$ -direction.  $E^a$  and  $p_z^a$  can be written in terms of  $E_T^a$  and  $y^a$  as

$$E^a = E_T^a \cosh y^a , \quad p_z^a = E_T^a \sinh y^a . \quad (2.3)$$

Since it is not possible to measure the neutrino momentum, one cannot directly determine the  $W$  invariant-mass from the experiment using eq.(2.1). Instead, one can consider the differential cross section of production of an electron-neutrino pair.

Let us start working in the CM system. Calling  $\theta, \phi$  the polar and azimuthal angles of the electron 3-momentum, the corresponding differential phase-space factor is proportional to the solid angle element  $d\sigma \propto d^2\Omega = d\cos\theta d\phi$ , where the integration over  $\phi$  can be performed in a trivial way using symmetry around the  $z$ -axis. Now, one can consider the distribution of cross section for different values of  $p_T^e$ , i.e.

$$d\sigma \propto \frac{d\cos\theta}{dp_T^e} dp_T^e , \quad (2.4)$$

where the Jacobian factor reads

$$\begin{aligned} \frac{d\cos\theta}{dp_T^e} &= \frac{-p_T^e |\vec{p}_e|}{\sqrt{|\vec{p}_e|^2 - (p_T^e)^2}} \\ &= \frac{-2E p_T^e |\vec{p}_e|}{\sqrt{E^2 - (E_T^e + E_T^\nu)^2} \sqrt{E^2 - (E_T^e - E_T^\nu)^2}} , \end{aligned} \quad (2.5)$$

with  $E = E^e + E^\nu$  denoting the total energy at CM ( $E = M_W$  if the  $W$  is produced on-shell). Of course the neutrino and electron masses are completely negligible in this context, but for future convenience we will maintain them in the expressions.

The phase-space factor (2.5) shows a *pole* at  $E_T^e + E_T^\nu = E$ . Denoting

$$\mathcal{E}_T = E_T^e + E_T^\nu = \sqrt{(p_T^e)^2 + m_e^2} + \sqrt{(p_T^\nu)^2 + m_\nu^2} \quad (2.6)$$

(which is  $\simeq 2p_T^e$  if  $m_e$  and  $m_\nu$  are neglected), one can change variables  $p_T^e \rightarrow \mathcal{E}_T$ , introducing a trivial Jacobian factor. So in the  $\mathcal{E}_T$  variable the pole occurs at

$$\mathcal{E}_T|_{\text{pole}} = E \simeq M_W . \quad (2.7)$$

In consequence, the histogram of events in the  $\mathcal{E}_T$  variable should show a peak at  $\mathcal{E}_T = E \sim M_W$  followed by an abrupt fall to zero, since  $\mathcal{E}_T \leq E$ , . This behavior is slightly softened by the fact that the  $W$  has a non-vanishing width.

The previous analysis was done at the CM system, but its extension to the LAB one is straightforward. First of all, since  $\mathcal{E}_T$  is invariant under  $z$ -boosts, the presence of the pole in  $\mathcal{E}_T$  at the CM energy ( $\simeq M_W$ ) holds in the LAB system assuming there is no net transverse momentum, which is a sensible approximation. Actually, this is a successful strategy to identify  $M_W$  in this context. Of course, in practice there can be a net transverse momentum if the collision is not completely along the  $z$ -line, due mainly to initial state radiation. To incorporate this effect to the analysis note that, in CM frame, the electron and neutrino momenta for *the events at the pole* have no longitudinal components, so that  $E_T^e = E^e$ ,  $E_T^\nu = E^\nu$ , and  $\mathcal{E}_T = E_T^e + E_T^\nu$  coincides with the total energy. These features obviously hold after a boost in a transverse direction. Consequently, in the boosted (LAB) system the pole in the cross section still occurs at

$$\mathcal{E}_T|_{\text{pole}} = E = \sqrt{E_{CM}^2 + (\vec{p}_T^e + \vec{p}_T^\nu)^2} , \quad (2.8)$$

where  $E_{CM} = M_W$ . (Of course the previous expression is invariant under further  $z$ -boosts.) If desired, the effect of a net transverse momentum of the  $W$  can be extracted by defining a “transverse mass”,  $M_T$ , as

$$\begin{aligned} M_T^2 &= \mathcal{E}_T^2 - (\vec{p}_T^e + \vec{p}_T^\nu)^2 = (E_T^e + E_T^\nu)^2 - (\vec{p}_T^e + \vec{p}_T^\nu)^2 \\ &\simeq 2 |p_T^e| |p_T^\nu| [1 - \cos(\phi^e - \phi^\nu)] , \end{aligned} \quad (2.9)$$

where in the last expression we have neglected the electron and neutrino masses, which is allowed in *this* context. Note that  $M_T$  is invariant under any boost and satisfies  $M_T \leq M_{\text{inv}}$ , so the cross section does present a pole at  $M_T = M_W$ . The complication is that the determination of  $\vec{p}_T^e + \vec{p}_T^\nu$  is not as clean as one would like (although normally is a subdominant term). Under the assumption of a perfect longitudinal collision, this term vanishes and  $M_T$  coincides with  $\mathcal{E}_T$ .

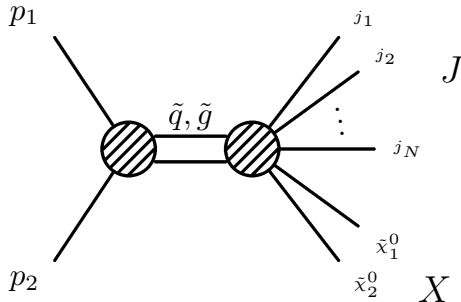


**Figure 2:** Diagram of production and decay of supersymmetric particles at LHC.

## 2.2 Pair production of SUSY particles at LHC

Now we consider our scenario of production of supersymmetric particles (in pairs) at the LHC. In most cases the supersymmetric particles produced are squarks and/or gluinos, which decay along jets through diverse channels, plus one lightest supersymmetric particle (LSP, usually a neutralino) for each SUSY particle. Therefore the final state mainly consists of jets (plus possibly some leptons) and two LSPs (plus possibly some neutrinos). This is schematically represented in Fig. 2, where we have not shown the fact that the decays occur along two chains, one for each initial supersymmetric particle. Normally the SUSY particles are created close to at-rest in the CM system, since producing them with substantial momentum amounts a high price from the parton distribution functions. Along the paper we will often use this approximation.

To connect with the strategy of the previous subsection, we can imagine that this process consists of the production of two pseudo-particles,  $J$  and  $X$ , which contain the jets and the two invisible LSPs respectively, as shown in Fig.2. Hence the momentum and the invariant mass of  $J$  ( $X$ ) is the global momentum and invariant mass of the set of jets (invisible particles). In this way, many of the results of the previous subsection can be applied here replacing the  $W$ -boson and its mass by the two initial supersymmetric particles and their global invariant mass,  $M_{\text{inv}}$ , or equivalently the total energy at CM; and replacing  $e \rightarrow J$ ,  $\nu \rightarrow X$ . The main difference with the  $W$ -case is that  $J$  and  $X$  have masses different from zero, which are equal to the invariant masses of the visible and invisible systems respectively. These masses, which change from event to event, may be quite large and cannot be neglected. In addition,  $M_{\text{inv}}$  does not coincide with the sum of the masses of the initial supersymmetric particles, since they are not produced exactly at rest, although this is normally a good approximation.

Now, working in the CM system, we can formally consider a subset of events with identical structure of jets and invisible particles, differing only in the  $\theta, \phi$  angles at which the pseudo-particle  $J$  (and thus  $X$ ) is produced. Obviously for those processes the phase space contains a factor like the one given in eq.(2.5), replacing  $e \rightarrow J$ ,  $\nu \rightarrow X$ . And this holds for any jet configuration. So we expect a similar pole in the  $\mathcal{E}_T$ -histogram. This can also be seen by performing a change of variables  $\vec{p}^1 \rightarrow \vec{p}^J = \sum_j \vec{p}^j$  in the phase space

integration of the jet momenta. One gets

$$\prod_{j=1}^N \frac{d^3 \vec{p}^j}{(2\pi)^3 2E^j} \rightarrow \frac{d^3 \vec{p}^J}{(2\pi)^3 2E^1} \prod_{j=2}^N \frac{d^3 \vec{p}^j}{(2\pi)^3 2E^j} \quad (2.10)$$

and a similar transformation for the momenta of the invisible particles. Then, in analogy with the  $W$ -case, we can now consider the differential cross section with respect to the transverse component of the  $J$ -momentum,  $p_T^J$ , obtaining that eqs.(2.4, 2.5) hold with the  $e \rightarrow J, \nu \rightarrow X$  replacements. Thus

$$d\sigma \propto \frac{d \cos \theta}{dp_T^J} dp_T^J, \quad (2.11)$$

where

$$\begin{aligned} \frac{d \cos \theta}{dp_T^J} &= \frac{-p_T^J |\vec{p}^J|}{\sqrt{|\vec{p}^J|^2 - (p_T^J)^2}} \\ &= \frac{-2E p_T^J |\vec{p}^J|}{\sqrt{E^2 - (E_T^J + E_T^X)^2} \sqrt{E^2 - (E_T^J - E_T^X)^2}} \end{aligned} \quad (2.12)$$

with  $E = E^J + E^X$  denoting the total energy in the CM and

$$\begin{aligned} E_T^J &= \sqrt{(p_T^J)^2 + m_J^2} = \sqrt{(E^J)^2 - (p_z^J)^2}, \\ E_T^X &= \sqrt{(p_T^X)^2 + m_X^2} = \sqrt{(E^X)^2 - (p_z^X)^2}. \end{aligned} \quad (2.13)$$

Again, we define a global ‘‘transverse energy’’ as

$$\mathcal{E}_T = E_T^J + E_T^X, \quad (2.14)$$

so that the differential cross section in the transverse momentum, eqs.(2.11, 2.12), shows a *pole* at

$$\mathcal{E}_T|_{\text{pole}} = E = M_{\text{inv}} \simeq m_1 + m_2. \quad (2.15)$$

Here  $m_1, m_2$  are the masses of the supersymmetric particles initially created, which, in the last identity, we have assumed to be produced approximately at rest in the CM system. This pole is maintained when the cross section is displayed in the  $\mathcal{E}_T$  variable because the change of variables  $p_T^J \rightarrow \mathcal{E}_T$  does not introduce any singular behavior. Note that the position of the pole is always the one given by eq.(2.15) for any subset of events (with any structure of jets and invisible particles) considered. So a global histogram in the  $\mathcal{E}_T$  variable must show a peak at  $\mathcal{E}_T = E \simeq m_1 + m_2$ . This is illustrated in Fig. 3, which shows the distribution of  $\mathcal{E}_T$  at CM compared with the invariant mass,  $M_{\text{inv}}$ , of the the supersymmetric particles initially produced. The plot corresponds to the benchmark point SU9 (defined and discussed in sect. 5) where for this particular example we have not included Initial State Shower. As one can see, the two histograms are pretty similar,

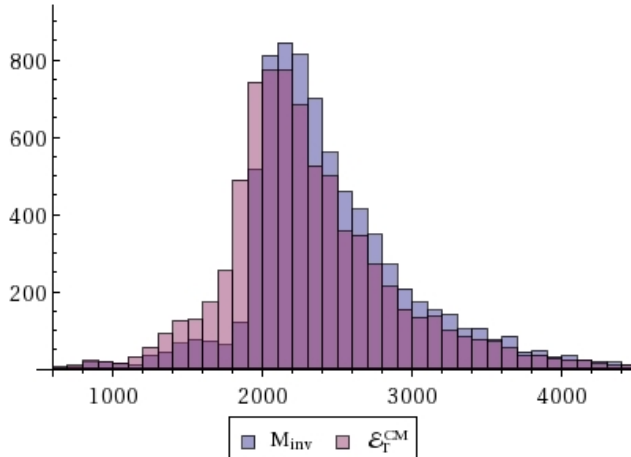


**Figure 3:**  $\mathcal{E}_T$  at CM frame (pink) compared with the global invariant mass,  $M_{\text{inv}}$ , of the supersymmetric particles initially produced (grey) for the benchmark point SU9 defined in sect. 5.

exhibiting a peak at the expected value. This similarity is mainly because  $J$  and  $X$  are normally rather heavy and therefore  $m_J$  and  $m_X$  are the dominant terms in the invariant mass, leading to a small contribution of  $p_z$ , even for events outside the pole.

We have indeed checked the presence of the peak at the expected value ( $\mathcal{E}_T \simeq m_1 + m_2$ ) for a large collection of CMSSM and more general MSSM models, using a PYTHIA simulation. This fact will be used in the next section to understand the correlation between  $M_{\text{susy}}$  and  $M_{\text{eff}}$ . We postpone the details and discussion of this and other related checks to section 5.

Since  $\mathcal{E}_T$  is invariant under boosts in the  $z$ -direction, the previous pole shows up also in the LAB system, provided the net transverse momentum of the two initial supersymmetric particles is small, which is the usual case. Once more, if desired, the effect of such net non-vanishing transverse momentum can be formally extracted by using, instead of  $\mathcal{E}_T$ , the transverse mass,  $M_T$ , defined as in eq.(2.9), i.e.  $M_T^2 = \mathcal{E}_T^2 - (\vec{p}_T^J + \vec{p}_T^X)^2$ .

### 3. Understanding the correlation $M_{\text{susy}} - M_{\text{eff}}$

In this section we show that the empirical correlation between  $M_{\text{eff}}$  (at the maximum of the histogram of events) and  $M_{\text{susy}}$  is an echo of the fact, discussed in the previous subsection, that the cross section has a pole (in practice a maximum) at  $\mathcal{E}_T \simeq m_1 + m_2$ .

Since the correlation has to do with the total mass of the two supersymmetric particles initially created, a convenient definition of  $M_{\text{susy}}$  is

$$M_{\text{susy}} = \frac{\sum_{a,b} \sigma_{ab} (m_a + m_b)}{\sum_{a,b} \sigma_{ab}}, \quad (3.1)$$

where  $a, b$  run over all supersymmetric particles and  $\sigma_{ab}$  is the production cross section of the  $\{a, b\}$  pair. Roughly speaking  $M_{\text{susy}}$  is the sum of the masses of the two supersym-

metric particles in the dominant channel of production. This definition is exactly twice the definition of  $M_{\text{susy}}$  proposed in ref.[16] and approximately twice the HPSSY definition given in eq.(1.2) if the dominant channel is squark-squark or gluino-gluino. In the rest of the paper  $M_{\text{susy}}$  will always refer to the definition of eq.(3.1)<sup>1</sup>.

Let us now discuss the definition and meaning of  $M_{\text{eff}}$ . Certainly  $M_{\text{eff}}$  has some resemblance with the  $\mathcal{E}_T$  variable defined in eqs.(2.14, 2.13). In order to deepen in the connection between both, let us re-write explicit expressions for the two variables.  $M_{\text{eff}}$  is defined as

$$M_{\text{eff}} = \sum_j |p_T^j| + |p_T^{\text{miss}}| \equiv M_{\text{eff}}^J + |p_T^{\text{miss}}|, \quad (3.2)$$

where for the sake of the discussion we have separated the jet contribution to the effective mass, denoted by  $M_{\text{eff}}^J$ , from the invisible one,  $|p_T^{\text{miss}}|$ . Normally  $M_{\text{eff}}^J$  is by far the most important contribution to  $M_{\text{eff}}$ . Note that we have slightly modified the initial definition of eq.(1.1) by extending the sum to all jets, rather than just the four hardest jets. This seems reasonable and follows the strategy of ref.[16]. A different thing is how to impose cuts in order to optimally count all the jets coming from the partonic process, leaving outside all the jets coming from initial state radiation. This will be addressed in sect. 5.

On the other hand,  $\mathcal{E}_T$ , defined in eqs.(2.14, 2.13), can be re-written in the following way

$$\mathcal{E}_T = E_T^J + E_T^X, \quad (3.3)$$

with

$$\begin{aligned} (E_T^J)^2 &= (E^J)^2 - (P_z^J)^2 \\ &= \sum_{j=1}^N \left( |\vec{p}_T^j|^2 + m_j^2 \right) + \sum_{i \neq j}^N \sqrt{|\vec{p}_T^i|^2 + m_i^2} \sqrt{|\vec{p}_T^j|^2 + m_j^2} \cosh(y_i - y_j), \end{aligned} \quad (3.4)$$

$$\begin{aligned} (E_T^X)^2 &= (E^X)^2 - (P_z^X)^2 \\ &= \sum_{\chi_i=1}^2 \left( |\vec{p}_T^{\chi_i}|^2 + m_{\chi_i}^2 \right) + 2 \sqrt{|\vec{p}_T^{\chi_1}|^2 + m_{\chi_1}^2} \sqrt{|\vec{p}_T^{\chi_2}|^2 + m_{\chi_2}^2} \cosh(y_{\chi_1} - y_{\chi_2}), \end{aligned} \quad (3.5)$$

where  $y_j$  and  $y_{\chi_{1,2}}$  are the rapidities of the jets and the two neutralinos (or whatever LSPs) respectively.

Comparing the above expressions (3.2)–(3.5) for  $M_{\text{eff}}$  and  $\mathcal{E}_T$  we see that  $M_{\text{eff}}^J \leq E_T^J$  and  $|p_T^{\text{miss}}| \leq E_T^X$ , so  $M_{\text{eff}} \leq \mathcal{E}_T$ . Focusing in  $M_{\text{eff}}^J$ , which is the main contribution to the effective mass, we see that the equality  $M_{\text{eff}}^J = E_T^J$  is only achieved when the jet masses are negligible, which is often a good approximation, and all jets have the same rapidity,  $y_i = y_j$ , which is trivially satisfied when there is only one jet, but for two or more jets is

---

<sup>1</sup>All these definitions may become problematic when the masses of the more frequently produced pairs of superparticles are very different. This instance will be discussed in sect. 5.

never satisfied in practice. Hence, using  $M_{\text{eff}}^J$  instead of  $E_T^J$  makes the peak of the histogram to occur systematically below  $m_1 + m_2$ .

We can go further by estimating how large is this effect in a typical case. Working in the CM system, the events corresponding to the peak of the histogram have  $p_z^J = 0$ . They satisfy  $E_T^J = E^J = \sum_j E^j \simeq \sum_j |\vec{p}^j|$ , where in the last equality we have neglected the jet masses. Consequently, at the peak of the histogram

$$\frac{M_{\text{eff}}^J}{E_T^J} \simeq \frac{\sum_j |p_T^j|}{\sum_j |\vec{p}^j|}. \quad (3.6)$$

Usually SUSY searches are done by considering events with a rather large number of jets, see e.g. refs.[13, 14, 17, 18]. Hence, for the sake of the estimate, a reasonable simplification is that (for the events at the peak of the histogram and working in CM) the directions of the various jets are distributed in a more-or-less random way. Then the differential probability that a jet occurs at a particular  $\theta$  is  $\sin\theta d\theta$ . In average  $\langle p_T^j \rangle = |\vec{p}^j| \int d\theta \sin^2\theta = (\pi/4)|\vec{p}^j|$ . Therefore, at the peak of the histogram

$$\frac{\langle M_{\text{eff}}^J \rangle}{E_T^J} \simeq \frac{\pi}{4} = 78.5\%. \quad (3.7)$$

This correlation is the main reason for the correlation found between  $M_{\text{eff}}$  at the peak of the histogram and  $\sim 80\% M_{\text{susy}}$ .

On the other hand, the  $|p_T^{\text{miss}}|$  contribution to the effective mass in eq.(3.2) is also systematically smaller than  $E_T^X$ , defined in eq.(3.5). As we will see in the next section and Appendix A, for events where the invisible particles are just two neutralinos with momenta larger than their masses, a more fair estimate for  $E_T^X$  is  $2|p_T^{\text{miss}}|$ . This means that the invisible contribution to the effective mass is around half the value suitable to get the peak of the histogram at  $m_1 + m_2$ .

We have numerically checked that the peak of the  $M_{\text{eff}}$  histogram is indeed around 70%–80%  $M_{\text{susy}}$ ; the precise value depends on the model and the cuts used in the analysis. This is illustrated by the statistical survey of CMSSM models presented in Fig. 5 below (light green crosses), which will be discussed in more detail in sect. 4.

#### 4. Proposal of a new kinematic variable, $\mathcal{E}_T^{\text{eff}}$

The discussion of the previous section not only allows to understand the correlation between  $M_{\text{eff}}$  and  $M_{\text{susy}}$ ; it also allows to propose an alternative variable which shows an even more robust correlation. As argued above, an histogram in  $\mathcal{E}_T$  shows a maximum near  $M_{\text{susy}}$ ; so the idea is simply to devise a new variable which is both measurable and as close as possible to  $\mathcal{E}_T$ .

Examining eqs.(3.3, 3.4, 3.5), we see that  $E_T^J$ , which is the dominant contribution to  $\mathcal{E}_T$ , can in principle be extracted directly from experiment.  $E_T^X$  cannot be deduced from the experiment, but is clearly larger than  $|p_T^{\text{miss}}|$  (the quantity used in the definition of

$M_{\text{eff}}$ ), unless the masses of the neutralinos are fairly smaller than their momenta *and* the latter have exactly aligned directions, which is unlikely. A much better estimate can be obtained by assuming that the relative directions of the two neutralinos are random in the CM system. This is exact if the the two initial supersymmetric particles are created at rest in CM. Under the further assumption that the 3-momenta of the two neutralinos are similar in magnitude and larger than the neutralino masses, it turns out that, in average,  $\langle E_T^X \rangle \simeq 2|p_T^{\text{miss}}|$ ; for more details see Appendix A. Thus our new kinematic variable, say  $\mathcal{E}_T^{\text{eff}}$ , simply reads

$$\mathcal{E}_T^{\text{eff}} = E_T^J + 2|p_T^{\text{miss}}|, \quad (4.1)$$

where  $E_T^J$  is given by eq.(3.4) or eq.(2.13). In the next section we will test the "performance" of  $\mathcal{E}_T^{\text{eff}}$  as a tool to determine  $M_{\text{susy}}$ , and compare it to that of  $M_{\text{eff}}$ ,

To finish this section, let us mention some of the a-priori advantages (and one disadvantage) of  $\mathcal{E}_T^{\text{eff}}$  with respect to  $M_{\text{eff}}$ . The most obvious advantage is that  $\mathcal{E}_T^{\text{eff}}$  is much closer to  $\mathcal{E}_T$ , and so we expect the peak of the corresponding histogram to be quite close to  $M_{\text{susy}}$  (which is in fact the case, as we will see). Notice that the definition of  $\mathcal{E}_T^{\text{eff}}$  (in particular the jet contribution,  $E_T^J$ ) contains information not only about the transverse components of the jet-momenta but also about the longitudinal ones, thus being more informative than  $M_{\text{eff}}$ . Actually,  $M_{\text{eff}}$  is proportional to  $\mathcal{E}_T$  only as an average, and the precise proportionality factor changes with analysis-dependent features, such as the number of jets considered for the selected events or the cuts performed on the various kinematical variables. Consequently the peak on the  $\mathcal{E}_T^{\text{eff}}$ -histogram is likely to indicate more faithfully the value of  $M_{\text{susy}}$  than the  $M_{\text{eff}}$ -one. Another important advantage of  $\mathcal{E}_T^{\text{eff}}$  is that it is robust under the procedure followed to identify the jets. Actually, as it is clear from eq. (2.13) or (3.4), for the definition of  $E_T^J$  we do not even need to talk about jets: we could perform the sum directly over hadronic final states; or we could consider all the hadronic particles as forming a single jet. The result is the same. On the other hand, a disadvantage of  $\mathcal{E}_T^{\text{eff}}$  with respect to  $M_{\text{eff}}$  is that it relies on a good knowledge of the longitudinal components of the jet momenta. E.g. one might dismiss a jet which really arises from the partonic event because it has large longitudinal component and does not pass the cut in rapidity. This would distort the estimated value of  $\mathcal{E}_T^{\text{eff}}$ . This happens also for  $M_{\text{eff}}$ , but in the latter case the contribution of such jets is less important, since only the transverse component is counted.

In consequence,  $\mathcal{E}_T^{\text{eff}}$  and  $M_{\text{eff}}$  are complementary variables, rather than competitors; and plotting histograms in both can be useful to cross-check the results, allowing a better and more robust identification of  $M_{\text{susy}}$ . The extension of this procedure to other scenarios of new physics (not necessarily SUSY) is also straightforward.

## 5. Testing the efficiency of $M_{\text{eff}}$ and $\mathcal{E}_T^{\text{eff}}$ in assorted SUSY models

We will discuss now the comparative behaviour of  $M_{\text{eff}}$  and  $\mathcal{E}_T^{\text{eff}}$ , and other kinematic variables, in the context of different MSSM models. We will simulate LHC signals at 14 TeV

center-of-mass energy using SOFTSUSY [19] and PYTHIA version 6.419 [20]. Focusing on events with multijets + missing transverse momentum, and applying the following cuts

1. At least three jets with  $p_T > 50$  GeV.
2. The hardest jet with  $p_T > 100$  GeV and  $|\eta| < 1.7$ .
3.  $p_T^{\text{miss}} > 100$  GeV.
4.  $\Delta\phi(\text{jet}_1 - p_T^{\text{miss}}) > 0.2$ ,  $\Delta\phi(\text{jet}_2 - p_T^{\text{miss}}) > 0.2$ ,  $\Delta\phi(\text{jet}_3 - p_T^{\text{miss}}) > 0.2$ .

For the evaluation of the various kinematic variables we will count all the jets (with  $p_T > 50$  GeV, as mentioned above)<sup>2</sup>. For the construction of the jets we will use FASTJET [21], with the antikt algorithm,  $E$  scheme and  $R = 0.4$ .

Let us start by illustrating the behavior of the various kinematic variables by considering a typical SUSY model, namely the benchmark point *SU9*, defined in ref. [12] and specified by the following values of the supersymmetric parameters:

$$m = 300 \text{ GeV}, \quad M_{1/2} = 425 \text{ GeV}, \quad A = 20, \quad \tan\beta = 20, \quad \mu > 0. \quad (5.1)$$

where  $m$ ,  $M_{1/2}$  and  $A$  are the universal scalar mass, gaugino mass and trilinear scalar coupling (all quantities defined at the  $M_X$  scale) respectively;  $\tan\beta \equiv v_2/v_1$  is the ratio between the vev's of the two Higgs doublets,  $H_1, H_2$ ; and  $\mu$  is the usual Higgs mass term in the superpotential, defined also at  $M_X$ . The corresponding values of the squark mass (first two generations) and the gluino mass are  $m_{\tilde{q}} = 920$  GeV,  $M_{\tilde{g}} = 994$  GeV. The corresponding value of  $M_{\text{susy}}$ , defined according to eq.(3.1), is

$$M_{\text{susy}} = 1898 \text{ GeV} . \quad (5.2)$$

Figure 4 (top-left panel) shows the histogram distributions of the invariant mass,  $M_{\text{inv}} = E_{CM}$ , and the histogram distribution of  $M_{\text{eff}}$ . Clearly the  $M_{\text{inv}}$  distribution shows a sharp starting point, almost coinciding with the maximum, at  $M_{\text{inv}} \simeq M_{\text{susy}}$ . Although the peak is quite sharp, the width of the distribution indicates to what extent the initial supersymmetric particles are created with non-vanishing momenta at CM. Of course  $M_{\text{inv}}$  is not directly measurable, so this histogram cannot be built in practice. On the other hand, the  $M_{\text{eff}}$ -histogram shows indeed a maximum correlated with  $M_{\text{susy}}$ , namely  $M_{\text{eff}} \simeq 70\% M_{\text{susy}}$  in this case. Figure 4 (top-right panel) shows the distribution of the  $\mathcal{E}_T$  variable compared with the  $M_{\text{inv}}$ -one. As expected from the discussion of sect. 2, the maximum of the two histograms are indeed very close. Comparing this with the  $\mathcal{E}_T^{\text{CM}}$  histogram, figure 3, one can see that  $\mathcal{E}_T$  is shifted to the left with respect to  $\mathcal{E}_T^{\text{CM}}$ . Note that now we are doing a more realistic simulation, including Initial State Shower (ISS), so, in order to avoid contamination from these ISS, one has to require jets with high  $p_T$  (as described above).

---

<sup>2</sup>We have checked (using a few SUSY points) the stability of  $\mathcal{E}_T^{\text{eff}}$  when applying a cut in  $\eta$ . Once one requires  $p_T > 50$  GeV, the impact of such cut is very small. The histograms are very similar whether one uses a  $|\eta| \lesssim 3$  cut or not cut at all.

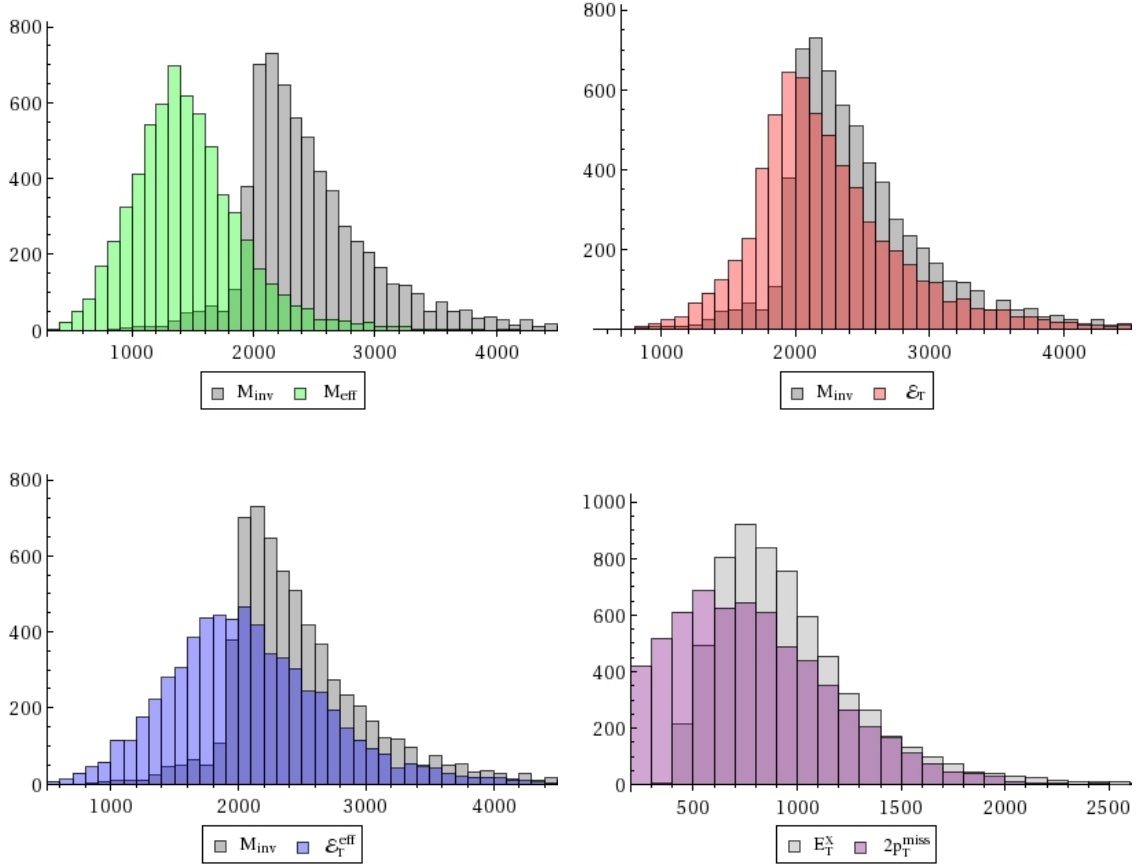


**Figure 4:**  $M_{\text{inv}}$  and  $M_{\text{eff}}$  (top-left panel),  $M_{\text{inv}}$  and  $\mathcal{E}_T$  (top-right panel),  $M_{\text{inv}}$  and  $\mathcal{E}_T^{\text{eff}}$  (bottom-left panel) and  $2|p_T^{\text{miss}}|$  and  $E_T^X$  (bottom-right panel) for the SU9 benchmark point.

Hence, the main reason for this shift is that by including those cuts we are losing some of the final particles coming from supersymmetric decays, which leads to an underestimate of the visible part; but still the maximum is where was expected. Fig 4 (bottom-left panel) is a similar plot, but using the measurable variable,  $\mathcal{E}_T^{\text{eff}}$ , defined in eq.(4.1). We see that the  $\mathcal{E}_T^{\text{eff}}$ -histogram maintains the peak close to  $M_{\text{susy}}$ , though is somewhat less sharp than in the  $\mathcal{E}_T$ -histogram. This is due to the fact that the invisible contribution to  $\mathcal{E}_T^{\text{eff}}$  in eq.(4.1), i.e.  $2|p_T^{\text{miss}}|$ , is an average of  $E_T^X$ , i.e. the actual contribution, to  $\mathcal{E}_T$ ; see eqs. (3.3, 3.5) and Appendix A. The goodness of such average (quite satisfactory in this case) can be appreciated in Figure 4 (bottom-right panel), where these two quantities are plotted.

Let us now explore how good is the behavior of  $M_{\text{eff}}$  and  $\mathcal{E}_T^{\text{eff}}$  in general SUSY models. We start considering a sample of 500 random CMSSM points requiring dominant  $\tilde{q}\tilde{q}$ ,  $\tilde{g}\tilde{q}$ ,  $\tilde{g}\tilde{g}$  production, which is the usual case. Recall that the CMSSM is defined by the values of

$$m, M_{1/2}, A, \tan\beta, \text{sign}\mu.$$

(Incidentally, the benchmark point *SU9*, defined at eq.(5.1) was a particular CMSSM model.) For all the models we have performed the simulation of the proton proton collisions

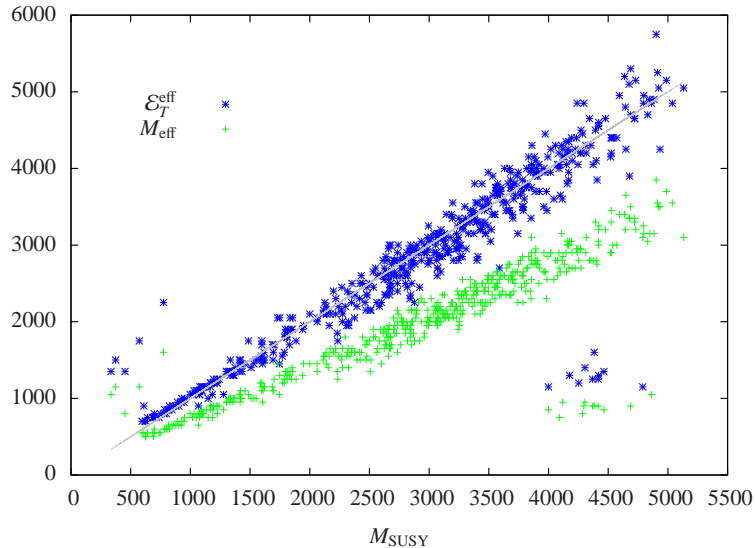


**Figure 5:**  $M_{\text{susy}}$  versus  $\mathcal{E}_T^{\text{eff}}$  (blue stars) and  $M_{\text{eff}}$  (light green crosses) for the CMSSM.

using the specifications presented at the beginning of this subsection.

Figure 5 shows the values of  $\mathcal{E}_T^{\text{eff}}$  (blue stars) and  $M_{\text{eff}}$  (light green crosses), which maximize their corresponding histograms, versus  $M_{\text{susy}}$  for those 500 CMSSM models.

As expected from the previous discussion, there is a remarkable correlation between  $\mathcal{E}_T^{\text{eff}}$  at the maximum of the histogram and  $M_{\text{susy}}$ ; namely  $\mathcal{E}_T^{\text{eff}} \simeq M_{\text{susy}}$ . The correlation is also good for the effective mass:  $M_{\text{eff}}$  (at the histogram maximum)  $\simeq 70\% M_{\text{susy}}$ , confirming the empirical observations of previous literature [15, 16].

Notice that, for large values of  $M_{\text{susy}}$ , there are few points which do not correlate well. This is because at large energies the production of charginos and neutralinos may become competitive. In that case there appear two separate peaks in the histograms, which makes the definition of  $M_{\text{susy}}$  fairly contrived.

Let us now extend the previous study to more general MSSM models, allowing non-universal soft parameters at the  $M_X$  scale. For that goal, we extend the previous parameter space, eq.(5), to a 15-dimensional parameter space, defined by

$$M_1, M_2, M_3; A_t, A_b, A_\tau; m_{H_u, H_d}; m_{\tilde{q}_L, \tilde{q}_R}, m_{\tilde{t}_L, \tilde{b}_L}, m_{\tilde{t}_R}, m_{\tilde{b}_R}; m_{\tilde{l}_L, \tilde{l}_R}, m_{\tilde{\tau}_L, \tilde{\nu}_{\tau L}}, m_{\tilde{\tau}_R}; \tan \beta.$$

Here  $M_a$  are the (non-universal) gaugino masses; and  $A_i, m_i$  are the non-universal trilinear scalar couplings and scalar masses ( $i$  denotes flavour species).  $\tilde{q}, \tilde{l}$  denote squarks and sleptons of the first two generations. As for the CMSSM case, we have studied 500 models chosen at random in this parameter space.

Figure 6 (left panel) is as Figure 5 but within this more general MSSM scenario. In this case the correlation is not as good as for the CMSSM, something that was empirically noticed in ref.[16] for the  $M_{\text{eff}}$  variable. We have checked that the reason is that now the neutralino masses can be much larger than in typical CMSSM models. Then, since

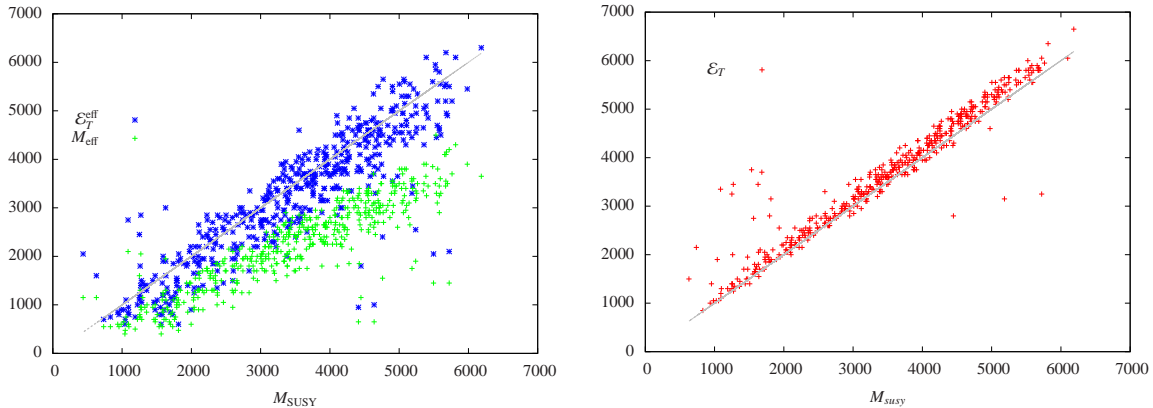


**Figure 6:** Left panel shows  $M_{\text{susy}}$  versus  $\mathcal{E}_T^{\text{eff}}$  (blue stars) and  $M_{\text{eff}}$  (light green crosses). Right panel shows  $M_{\text{susy}}$  versus  $\mathcal{E}_T$  (red crosses). Both for the MSSM.

in the definition of both  $M_{\text{eff}}$  and  $\mathcal{E}_T^{\text{eff}}$  one is neglecting the neutralino masses, one is missing a potentially important piece. Furthermore, in some cases many neutrinos can be produced. This makes the average missing transverse energy,  $E_T^X$ , larger than the average  $\simeq 2|p_T^{\text{miss}}|$  used in the definition of  $\mathcal{E}_T^{\text{eff}}$  (and of course larger than the  $|p_T^{\text{miss}}|$  piece entering the definition of  $M_{\text{eff}}$ ). This can be checked by plotting the true  $\mathcal{E}_T$  variable (which cannot be directly measured). This has been done in the right panel of figure 6. Remarkably, here the correlation with  $M_{\text{susy}}$  is nicely maintained, indicating that the spreading exhibited by  $\mathcal{E}_T^{\text{eff}}$  and  $M_{\text{eff}}$  is indeed due to an underestimate of the invisible contribution.

The previous discussion suggests that a better correlation could be found by refining the estimate  $\langle E_T^X \rangle \simeq 2|p_T^{\text{miss}}|$  used above, by taking into account the finite size of neutralino masses. As discussed at the end of the Appendix, a more refined estimate of the invisible transverse energy for the events at the pole is obtained by retaining the dominant terms in  $m_\chi^2$ , and reads  $\langle E_T^X \rangle \simeq \sqrt{4(p_T^X)^2 + 4m_\chi^2} \simeq 2p_T^X + 2m_\chi^2/E_T^X$ . Using the fact that typically  $E_T^X$  contributes less than half to  $\mathcal{E}_T$ , we get a conservative correction  $\sim 4m_\chi^2/M_{\text{susy}}$  to  $\mathcal{E}_T^{\text{eff}}$  for the events at the pole. Alternative, we can keep the definition of  $\mathcal{E}_T^{\text{eff}}$  given at eq. (4.1). Then the value of  $\mathcal{E}_T^{\text{eff}}$  at the maximum of the histogram must be around

$$M_{\text{susy}} - 4 \frac{m_\chi^2}{M_{\text{susy}}} , \quad (5.3)$$

rather than  $M_{\text{susy}}$ . Incidentally, a similar correction to  $M_{\text{susy}}$  with the same functional dependence but half the value, was proposed in ref.[16].

Fig. 7 shows  $M_{\text{susy}} - 4 \frac{m_\chi^2}{M_{\text{susy}}}$  versus  $\mathcal{E}_T^{\text{eff}}$  for the same 500 general MSSM models displayed in Fig. 6. Clearly the correlation is now much better, comparable to that found for CMSSM models (Fig. 6). The correction (5.3) can also be applied to CMSSM models, but in that case the improvement is less significant since  $m_\chi$  is normally much smaller than  $M_{\text{susy}}$ .

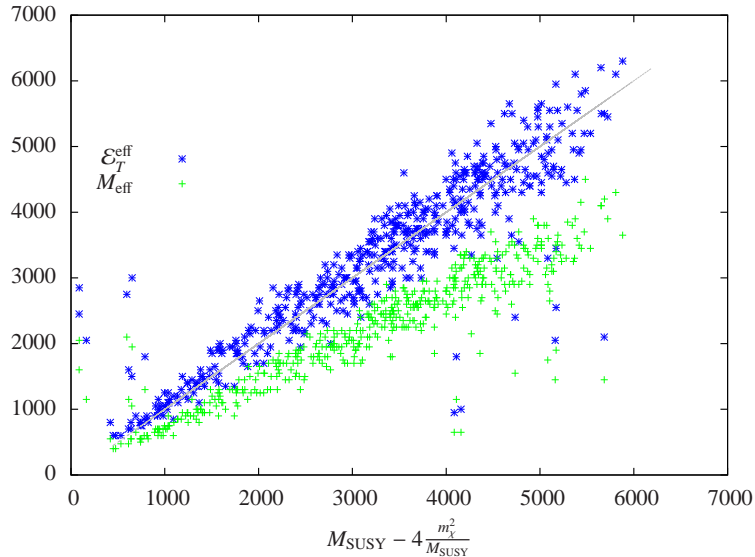


**Figure 7:**  $M_{\text{susy}} - 4 \frac{m_{\chi}^2}{M_{\text{susy}}}$  versus  $\mathcal{E}_T^{\text{eff}}$  (blue stars) and  $M_{\text{eff}}$  (light green crosses) for the MSSM.

## 6. Conclusions

There is an intense activity to explore assorted strategies for the search of new physics at the LHC. A paradigmatic case is supersymmetry (SUSY). Under the assumption that superparticles are light enough to be produced and detected at LHC, one can expect a typical signal of multijets and large missing energy. However, the analysis is quite complicated and the correct identification and reconstruction of the properties of the final states is quite tough. Besides, the separation of the decay chains is normally not possible. In this context the use of appropriate kinematic variables is instrumental to maximize the signal of new physics from the Standard Model background.

A handy and extensively used kinematic variable, e.g. in ATLAS analyses, is the Effective Mass variable, defined as

$$M_{\text{eff}} = \sum_j |p_T^j| + |p_T^{\text{miss}}| \equiv M_{\text{eff}}^J + |p_T^{\text{miss}}|. \quad (6.1)$$

It was empirically found in refs.[15, 16] that for the Constrained Minimal Supersymmetric Standard Model (CMSSM) there is an outstanding correlation between the value of  $M_{\text{eff}}$  at which the histogram of events has a maximum and the typical supersymmetric masses. Namely,

$$M_{\text{eff}}|_{\text{max}} \simeq 80\% M_{\text{susy}}, \quad (6.2)$$

where  $M_{\text{susy}} \sim m_1 + m_2$ , i.e. the sum of the masses of the supersymmetric particles initially created (usually squark-squark, gluino-gluino or squark-gluino). However, for some points in the CMSSM, and especially in the general MSSM, the correlation fails.

In this paper we have found an explanation for the above correlation (6.2). We have argued that  $M_{\text{eff}}$  is typically 80% of a kinematic variable,  $\mathcal{E}_T$ , defined as the sum of the

transverse energies of the visible and the invisible parts of the decay products of the initial supersymmetric particles; for more details see eqs.(2.13) and (3.4, 3.5). Then it can be shown that, at CM, the cross section has a maximum at  $\mathcal{E}_T = E_{\text{CM}} \sim m_1 + m_2$ . This relation is invariant under longitudinal boosts and thus is kept as a good approximation in the LAB frame.

This understanding has allowed us to propose a new kinematic variable, the effective transverse energy  $\mathcal{E}_T^{\text{eff}}$ , which is measurable and as close as possible to  $\mathcal{E}_T$ . It reads

$$\mathcal{E}_T^{\text{eff}} = E_T^J + 2|p_T^{\text{miss}}|. \quad (6.3)$$

where  $(E_T^J)^2 = (E^J)^2 - (p_z^J)^2$  is the hadronic transverse energy [for more details see eqs.(2.13), (3.4)].  $\mathcal{E}_T^{\text{eff}}$  is a kinematic variable alternative to  $M_{\text{eff}}$ , which shows an even better and more direct correlation with the supersymmetric mass

$$\mathcal{E}_T^{\text{eff}} \Big|_{\text{max}} \simeq M_{\text{susy}}. \quad (6.4)$$

Besides,  $\mathcal{E}_T^{\text{eff}}$  has other advantages, like being more robust under the procedure followed to identify the jets (actually, it is completely independent of it). On the other side, the determination of  $\mathcal{E}_T^{\text{eff}}$  relies (more than for  $M_{\text{eff}}$ ) on a good knowledge of the longitudinal components of the jet momenta. In consequence,  $\mathcal{E}_T^{\text{eff}}$  and  $M_{\text{eff}}$  are complementary variables, rather than competitors; and plotting histograms in both can be useful to cross-check the results, allowing a better and more robust identification of  $M_{\text{susy}}$ . The extension of this procedure to other scenarios of new physics (not necessarily SUSY) is also straightforward.

We have shown these features in the context of the CMSSM or more general MSSM models by examining the above correlations in a large number of points in the parameter space. The results show that  $\mathcal{E}_T^{\text{eff}}$  is a simple and valuable kinematic variable to determine the characteristic supersymmetric masses.

Our analysis also shows why the above correlations fail for some models. This is because at large energies the production of charginos and neutralinos may become competitive. In those cases there appear two separate peaks in the histograms, which makes the previous analysis too simple. In addition, for general MSSM models (departing from the conventional CMSSM) the neutralino masses can be much larger than in typical CMSSM models. Furthermore, in some cases many neutrinos can be produced. In those cases, the term representing the missing transverse energy in (6.1) and even in (6.3) underestimates the actual invisible contribution and a more refined estimate of it must be used. Then, retaining the dominant contributions in the neutralino mass, the right-hand side of eq. (6.4) gets shifted as  $M_{\text{susy}} \rightarrow M_{\text{susy}} - 4m_\chi^2/M_{\text{susy}}$ , significantly improving the correlation.

## 7. Appendix

In this appendix we evaluate the average value of the missing transverse energy, defined in eq.(2.13),

$$(E_T^X)^2 = (p_T^X)^2 + m_X^2 = (E^X)^2 - (p_z^X)^2. \quad (7.1)$$

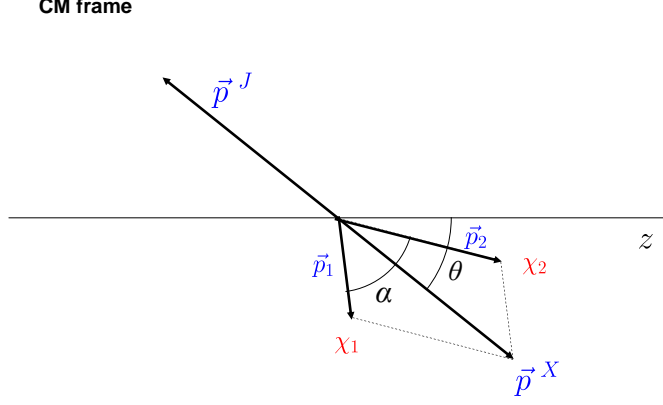


**Figure 8:**

Here  $p_T^X$ ,  $p_z^X$  are the transverse and longitudinal components of the total invisible 4-momentum

$$p^X = p_1 + p_2 , \quad (7.2)$$

where  $p_1, p_2$  are the two 4-momenta of the two final-state neutralinos,  $\chi_1, \chi_2$ . From now on we will work in the CM reference frame, see Fig.8. As represented in Fig.8,  $\theta$  denotes the angle of  $\vec{p}^X$  with the longitudinal axis,  $z$ ; and  $\alpha$  the angle between  $\vec{p}_1$  and  $\vec{p}_2$ . Let us now write the missing energy,  $E_T^X$ , using the second equality in eq.(7.1):

$$\begin{aligned} (E_T^X)^2 &= \left( \sqrt{\vec{p}_1^2 + m_\chi^2} + \sqrt{\vec{p}_2^2 + m_\chi^2} \right)^2 - (\vec{p}^X)^2 \cos^2 \theta \\ &= 2m_\chi^2 + 2\sqrt{(\vec{p}_1^2 + m_\chi^2)(\vec{p}_2^2 + m_\chi^2)} + (\vec{p}_1^2 + \vec{p}_2^2) \sin^2 \theta - 2|\vec{p}_1||\vec{p}_2| \cos \alpha \cos^2 \theta. \end{aligned} \quad (7.3)$$

On the other hand, the invisible transverse momentum,  $p_T^X$ , is given by

$$(p_T^X)^2 = (\vec{p}_1^2 + \vec{p}_2^2) \sin^2 \theta + 2|\vec{p}_1||\vec{p}_2| \cos \alpha \sin^2 \theta . \quad (7.4)$$

Hence,

$$(E_T^X)^2 = (p_T^X)^2 + 2m_\chi^2 + 2\sqrt{(\vec{p}_1^2 + m_\chi^2)(\vec{p}_2^2 + m_\chi^2)} - 2|\vec{p}_1||\vec{p}_2| \cos \alpha . \quad (7.5)$$

This expression admits further simplifications under some reasonable assumptions. Assuming  $m_\chi^2 \ll (\vec{p}_i)^2$ , we have

$$(E_T^X)^2 \simeq (p_T^X)^2 + 2|\vec{p}_1||\vec{p}_2|(1 - \cos \alpha) = (p_T^X)^2 \left[ 1 + \frac{2|\vec{p}_1||\vec{p}_2|(1 - \cos \alpha)}{\sin^2 \theta (\vec{p}_1^2 + \vec{p}_2^2 + 2|\vec{p}_1||\vec{p}_2| \cos \alpha)} \right] \quad (7.6)$$

Finally, we can assume that typically  $|\vec{p}_1| \sim |\vec{p}_2|$ . Then

$$(E_T^X)^2 \simeq (p_T^X)^2 \left[ 1 + \frac{1 - \cos \alpha}{\sin^2 \theta (1 + \cos \alpha)} \right] . \quad (7.7)$$

Now, we can single out the previous expression for the events at the pole, i.e. with  $\theta = \pi/2$ . Notice also that, assuming that the initial supersymmetric particles are approximately at rest, it turns out that the relative directions of  $\vec{p}_1$  and  $\vec{p}_2$  are random, so the differential probability for a particular value of the angle  $\alpha$  is  $\mathcal{P}(\alpha) = \frac{1}{2} \sin \alpha d\alpha$ . In conclusion

$$\langle E_T^X \rangle_{\text{pole}} \simeq \frac{1}{2} p_T^X \int_0^\pi d\alpha \sin \alpha \left[ 1 + \frac{1 - \cos \alpha}{1 + \cos \alpha} \right]^{1/2} = 2 p_T^X, \quad (7.8)$$

which is the estimate used of  $E_T^X$  throughout most of the paper. The goodness of this approximation is illustrated in Fig.4 (bottom-right panel) for a typical example.

A more refined estimate can be obtained by keeping the dominant terms in  $m_\chi^2$  in eq. (7.5). Then, eq. (7.8) gets slightly modified:

$$\langle E_T^X \rangle_{\text{pole}} \simeq \sqrt{4(p_T^X)^2 + 4m_\chi^2}. \quad (7.9)$$

## Acknowledgements

We are extremely grateful to Juan Terrón for illuminating discussions and his help with statistical tools. Likewise we thank Agustín Sabio, Roberto Ruiz de Austri, Gianfranco Bertone and Paul de Jong for interesting discussions and suggestions.

This work has been partially supported by the MICINN, Spain, under contract FPA2010-17747; Consolider-Ingenio PAU CSD2007-00060, CPAN CSD2007-00042. We thank as well the Comunidad de Madrid through Proyecto HEPHACOS S2009/ESP-1473 and the European Commission under contract PITN-GA-2009-237920. M. E. Cabrera acknowledges the financial support of the CSIC through a predoctoral research grant (JAEPRe 07 00020); and the ERC “WIMPs Kairos - the moment of truth for wimp dark matter” (P.I. Gianfranco Bertone).

## References

- [1] C. Lester and D. Summers, *Measuring masses of semiinvisibly decaying particles pair produced at hadron colliders*, *Phys.Lett.* **B463** (1999) 99–103, [[hep-ph/9906349](#)].
- [2] A. Barr, C. Lester, and P. Stephens, *m(T2): The Truth behind the glamour*, *J.Phys.G* **G29** (2003) 2343–2363, [[hep-ph/0304226](#)].
- [3] C. Lester and A. Barr, *MTGEN: Mass scale measurements in pair-production at colliders*, *JHEP* **0712** (2007) 102, [[arXiv:0708.1028](#)].
- [4] W. S. Cho, K. Choi, Y. G. Kim, and C. B. Park, *Gluino Stransverse Mass*, *Phys.Rev.Lett.* **100** (2008) 171801, [[arXiv:0709.0288](#)].
- [5] A. J. Barr, B. Gripaios, and C. G. Lester, *Weighing Wimps with Kinks at Colliders: Invisible Particle Mass Measurements from Endpoints*, *JHEP* **0802** (2008) 014, [[arXiv:0711.4008](#)].
- [6] M. Burns, K. Kong, K. T. Matchev, and M. Park, *Using Subsystem MT2 for Complete Mass Determinations in Decay Chains with Missing Energy at Hadron Colliders*, *JHEP* **0903** (2009) 143, [[arXiv:0810.5576](#)].

- [7] L. Randall and D. Tucker-Smith, *Dijet Searches for Supersymmetry at the LHC*, *Phys.Rev.Lett.* **101** (2008) 221803, [[arXiv:0806.1049](#)].
- [8] G. Polesello and D. R. Tovey, *Supersymmetric particle mass measurement with the boost-corrected contranverse mass*, *JHEP* **1003** (2010) 030, [[arXiv:0910.0174](#)].
- [9] W. S. Cho, J. E. Kim, and J.-H. Kim, *Amplification of endpoint structure for new particle mass measurement at the LHC*, *Phys.Rev.* **D81** (2010) 095010, [[arXiv:0912.2354](#)].
- [10] I.-W. Kim, *Algebraic Singularity Method for Mass Measurement with Missing Energy*, *Phys.Rev.Lett.* **104** (2010) 081601, [[arXiv:0910.1149](#)].
- [11] P. Konar, K. Kong, K. T. Matchev, and M. Park, *Superpartner Mass Measurement Technique using 1D Orthogonal Decompositions of the Cambridge Transverse Mass Variable  $M_{T2}$* , *Phys.Rev.Lett.* **105** (2010) 051802, [[arXiv:0910.3679](#)].
- [12] **The ATLAS Collaboration**, G. Aad et al., *Expected Performance of the ATLAS Experiment - Detector, Trigger and Physics*, [arXiv:0901.0512](#).
- [13] **Atlas Collaboration** Collaboration, G. Aad et al., *Search for squarks and gluinos using final states with jets and missing transverse momentum with the ATLAS detector in  $\sqrt{s} = 7$  TeV proton-proton collisions*, *Phys.Lett.* **B701** (2011) 186–203, [[arXiv:1102.5290](#)].
- [14] **ATLAS Collaboration** Collaboration, G. Aad et al., *Search for squarks and gluinos using final states with jets and missing transverse momentum with the ATLAS detector in  $\sqrt{s} = 7$  TeV proton-proton collisions*, *Phys.Lett.* **B710** (2012) 67–85, [[arXiv:1109.6572](#)].
- [15] I. Hinchliffe, F. Paige, M. Shapiro, J. Soderqvist, and W. Yao, *Precision SUSY measurements at CERN LHC*, *Phys.Rev.* **D55** (1997) 5520–5540, [[hep-ph/9610544](#)].
- [16] D. R. Tovey, *Measuring the SUSY mass scale at the LHC*, *Phys. Lett.* **B498** (2001) 1–10, [[hep-ph/0006276](#)].
- [17] **Atlas Collaboration** Collaboration, G. Aad et al., *Search for new phenomena in final states with large jet multiplicities and missing transverse momentum using  $\sqrt{s}=7$  TeV pp collisions with the ATLAS detector*, *JHEP* **1111** (2011) 099, [[arXiv:1110.2299](#)].
- [18] **ATLAS Collaboration** Collaboration, G. Aad et al., *Hunt for new phenomena using large jet multiplicities and missing transverse momentum with ATLAS in  $4.7 \text{ fb}^{-1}$  of  $\sqrt{s} = 7$  TeV proton-proton collisions*, [arXiv:1206.1760](#).
- [19] B. Allanach, *SOFTSUSY: a program for calculating supersymmetric spectra*, *Comput.Phys.Commun.* **143** (2002) 305–331, [[hep-ph/0104145](#)].
- [20] T. Sjostrand, S. Mrenna, and P. Z. Skands, *PYTHIA 6.4 Physics and Manual*, *JHEP* **0605** (2006) 026, [[hep-ph/0603175](#)].
- [21] M. Cacciari, G. P. Salam, and G. Soyez, *FastJet user manual*, [arXiv:1111.6097](#).